IEEE Access
Multidisciplinary ⋮ Rapid Review ⋮ Open Access Journal

Received February 27, 2021, accepted March 17, 2021, date of publication March 22, 2021, date of current version March 29, 2021.

Digital Object Identifier 10.1109/ACCESS.2021.3067637

Selective Laser Sintering Manufacturing as a Low Cost Alternative for Flat-Panel Antennas in Millimeter-Wave Bands

MIGUEL FERRANDO-ROCHER[1,2], (Member, IEEE), JOSE IGNACIO HERRANZ-HERRUZO[1], (Member, IEEE), ALEJANDRO VALERO-NOGUEIRA[1], (Senior Member, IEEE), AND BERNARDO BERNARDO-CLEMENTE[1]

[1]Antennas and Propagation Laboratory (APL), Universitat Politecnica de València (UPV), 46022 València, Spain
[2]Microwave and Applied Computational Electromagnetics Group (GMECA), Universidad de Alicante (UA), 03690 Alicante, Spain

Corresponding author: Miguel Ferrando-Rocher (miguel.ferrando@ua.es)

This work was supported by the Spanish Ministry of Economy and Competitiveness (Ministerio de Economía y Competitividad) under Project PID2019-107688RB-C22.

ABSTRACT In this paper, the capabilities of Selective Laser Sintering metal 3D-Printing technology to achieve a lightweight and cost-effective flat panel antenna in the millimeter wave band are studied. Specifically, two identical dual-band 4 × 4 array antennas working in the K and Ka bands have been manufactured; one with Selective Laser Sintering (SLS) and one using computer numerical control (CNC). Measured performance of the SLS antenna prototype is benchmarked with the performance of the previously measured CNC antenna. Experimental results reveal the strengths and weaknesses of this particular low-cost additive manufacturing technique with respect to traditional subtractive manufacturing techniques.

INDEX TERMS Additive manufacturing, high-efficiency wideband single-layer antenna array, Ka-band, selective metal laser sintering, SLS technique, aluminum alloy, substractive manufacturing.

I. INTRODUCTION

Additive manufacturing (AM) provided by different three-dimensional (3D) printing systems increases the degrees of freedom in device design, enabling complex 3D structures built from a variety of materials. Especially in antenna applications, where geometry is crucial for the radiation performance, AM unleashes vast potential and it has been increasingly considered by several scientific and even commercial applications [1]. Realizations of several millimeter-wave band antennas and components using 3D printing and subsequent metal plating have been recently reported in the literature, for example, horn arrays [2], [3], slot arrays [4], [5] or waveguide antenna arrays [6]–[8]. In addition, a very complete review of the state of the art of 3D antennas can be found in [9]. From this recent contribution, it is observed that very few millimeter-wave arrays have been fabricated using metallic additive manufacturing.

The associate editor coordinating the review of this manuscript and approving it for publication was Debdeep Sarkar.

Selective Laser Sintering (SLS) allows for the direct fabrication of metal parts by layer-wise melting of metal powder, i.e., there is no need of a support. On the one hand, the piece is supported directly by friction and cohesion with the surrounding dust which gives a total design freedom. On the other hand, because the technology requires a high power laser, the SLS machines are unsafe to operate in a smaller space than a workshop. Besides, finished pieces tend to exhibit rough and grainy surfaces.

Therefore, to study the feasibility of using this low-cost AM technique in the context of mm-wave flat panel antennas, this contribution presents the performance of an SLS gap waveguide 4 × 4 array antenna working simultaneously in the K and Ka bands. An in-depth study is made of its characteristics, measurements and manufacturing dimensions, and they are compared to those obtained in an identical mechanized antenna in CNC, which is used as a reference frame [10]. Fabricated pieces of both samples are shown in Fig. 1a.

So, next sections are organized as follows. Section II provides a preliminary consideration of the design of the manufactured antenna. Section III presents a brief review of

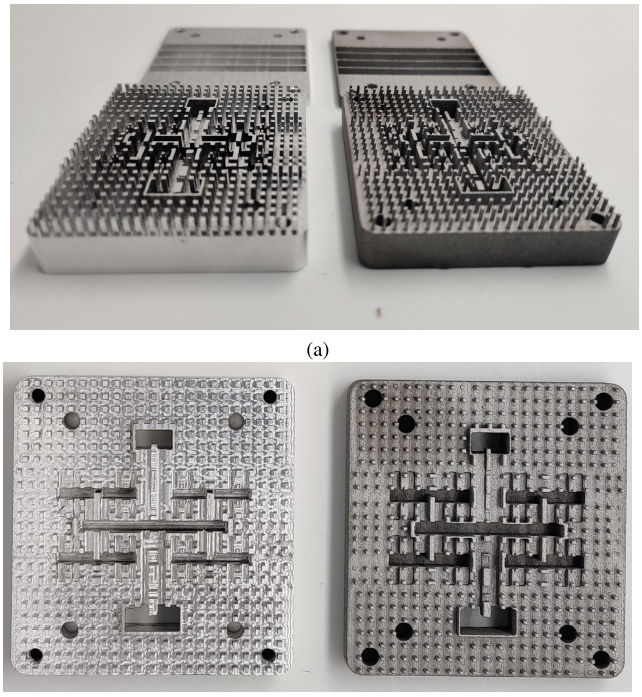

FIGURE 1. (a) Photographs of the antennas without cover. The left one is made with CNC machining, the right one with SLS, and (b) top view of the bottom pieces.

AM techniques and in Section IV the metrological study of the prototype conducted on both the SLS and CNC antennas is described. Section V shows the experimental results of the SLS antenna and they are compared with the mechanized antenna measured performance. Finally, Section VI discusses the advantages and disadvantages of the SLS technology for use in flat panel antennas in the mm-wave band. Conclusions are presented in Section VII.

II. PREVIOUS CONSIDERATIONS OF THE ANTENNA DESIGN

The Gap-Waveguide (GW) technology, which emerged in 2008 [11], is especially useful in the millimeter-wave band since permits the fabrication of low-loss structures without requiring perfect contact between metallic pieces. Therefore, the field leakage problem, typically present when miniaturizing devices in the millimeter-wave band, is minimized. Gap waveguide based mm-wave antennas have reported higher efficiencies when compared to similar antennas implemented in other technologies, such as SIW or LTCC (Low Temperature Co-fired Ceramic) [12]. So, the main difference between gap waveguides and conventional waveguides lies in the fact that metallic pieces do not need to have an electrical contact with each other, still ensuring the confinement of the field within the structures.

The theoretical design of the coaxial cavities on which the antenna under study is based can be consulted in more detail in [13], [14]. In particular, the work presented in [15] provides a very complete and theoretical review of the resonance generated around a shortened cylindrical nail which is fed through Groove Gap Waveguides (GGW).

The first challenge in antenna design was to modify the coaxial cavity in order to resonate at two very separate working bands. The second challenge was to design a corporate-feed network compact enough to place the slots as close together as physically possible to avoid grating lobes. Thus, this antenna is mainly based on the proper combination of two components: a very compact network combining two different types of gap waveguides [16], and dual-mode cavity resonators backing I-shaped slots. Further details and analysis of this antenna and all its dimensions can be consulted in [10], focused exclusively on a mechanized prototype.

III. BRIEF REVIEW OF ADDITIVE MANUFACTURING TECHNIQUES

First of all, it is necessary to clarify the multiple terms that usually appear in documents referring to additive manufacturing techniques. Typically, these include SLA, PolyJet, SLM, DMLS or SLS.

Stereolithography (SLA) uses the principle of photopolymerization to create 3D models from UV-sensitive resins. Similar to SLA is the polymer jetting technique (Polyjet), which also uses liquid photopolymers that are hardened by exposure to an ultraviolet laser. One main difference is that SLA printers use vat polymerization technologies with far more heat than PolyJet, which uses lower temperatures.

In Selective Laser Melting (SLM) a high-powered laser fully melts each layer of metal powder. Selective laser melting produces printed objects that are extremely dense and strong. Currently, SLM is mainly used with certain metals as titanium, cobalt, chrome or aluminum. Finally, the techniques known as Selective Laser Sintering (SLS) and Direct Metal Laser Sintering (DMLS) use a focused laser beam, that, on a molecular level, sinters the powder together (it do not melt it). While SLS can be used with a variety of metals and non-metallic materials, DMLS is designed to work solely with metals.

Compared to SLA, SLS does not require support structures since the powder acts as a self-supporting material. This allows intricate and complex geometries to be constructed, with an almost complete design freedom. This fact, together with the scarcity of SLS antenna prototypes in the literature, has been the reason for choosing this manufacturing technique in this research.

IV. METROLOGICAL STUDY

A K-Ka Dual-Band antenna array has been fabricated by an SLS process employing metal alloy (Aluminum AlSi10Mg). The antenna under study consists of a 4×4 single-layer dual-band array using GW technology. As aforementioned, the radiating elements consist of I-shaped slots (Fig. 2), cavity backed by dual-mode resonators fed by a unique broadband corporate-feed network. The description of the elements that make up this design and the performance of the mechanized prototype were presented in [10]. Now, a new prototype in

TABLE 1. Metrological study of the prototypes manufactured with SLS and CNC (dimensions in mm).

-	w_{d30}	w_{d20}	w_p	h_p	w_{p2}	h_{p2}	h_{GGW}	w_{GGW}	w_{RGW}	h_{RGW}	w_a	w_b	l_a	l_b
Design	1	1.5	0.9	3	0.9	3	8.47	2.12	1	7.1	1.17	2.64	6.12	1.03
CNC (fabricated)	1.00	1.51	0.91	3.01	0.89	3.04	8.52	1.96	1.01	7.13	1.16	2.64	6.13	1.01
SLS (fabricated)	0.75	1.26	0.62	3.06	0.67	3.04	8.51	2.33	0.80	7.16	1.39	2.88	5.89	1.23
$error_{CNC}$ (μm)	0	10	10	10	10	40	50	160	10	20	10	0	10	20
$error_{SLS}$ (μm)	250	240	280	60	230	40	40	210	200	60	220	240	230	200

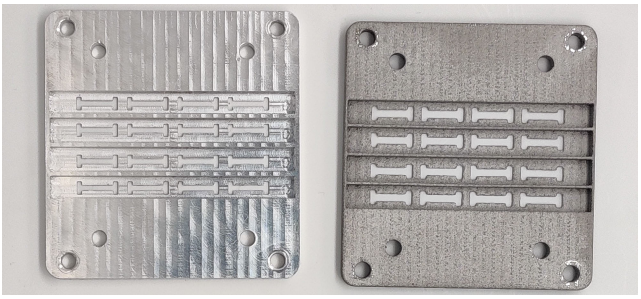

FIGURE 2. Photographs of the radiating layer. The left one is made with CNC machining, the right one with SLS.

additive technology has been manufactured. The objective of this paper is not so much to discuss the antenna presented in [10], but to use it as a reference to analyze the advantages and disadvantages of its replication in additive technology.

The SLS piece was ordered from the company Protolabs. In its specification sheet, Protolabs advises that the maximum size of the piece to manufacture in SLS technique cannot be larger than 200mm×200mm×200mm. Larger sizes may increase the risk of deformation and/or dimensional inaccuracy. Furthermore, the tolerances typically provided by the manufacturer give a margin of ± 0.35 mm, being the minimum wall thickness of 1 mm. As for the standard finishing, it consists of a shot blasting to remove all the remaining dust, which in principle should leave a uniform overall texture. The mechanized piece was in-house manufactured in the facilities of the Antennas and Propagation Laboratory in UPV. The assured tolerances were ±15 μm in the horizontal plane and 50 μm in the vertical dimension.

Table 1 presents a summary of the metrological study carried out. It provides the ideal design dimensions and those measured in the manufactured prototypes. The dimensions under study have been chosen for their critical character in antenna performance: w_{d30} and w_{d20} refer to the width of the resonators used in the antenna input filters; w_p, h_p refer to the nail width and height in the bed of nails. Note that sub-index 2 refers to a different nail of the bed to study the repeatability. h_{GGW} and w_{GGW} refer to the height and width of the GGW [17]. For the Ridge Gap Waveguide (RGW) dimensions the sub-index RGW is used instead. Finally, the last four parameters in the table refer to the lengths and widths of the radiating elements. Fig. 4 illustrates and indicates these dimensions for better identification of the elements.

An observed fact and not a minor one for the piece manufactured in SLS is that nails are thinner than those of the machined piece. The metrological measurement confirms an average nail width of 0.65 mm, instead of the expected 0.9 mm. This manufacturing deviation, which is obviously

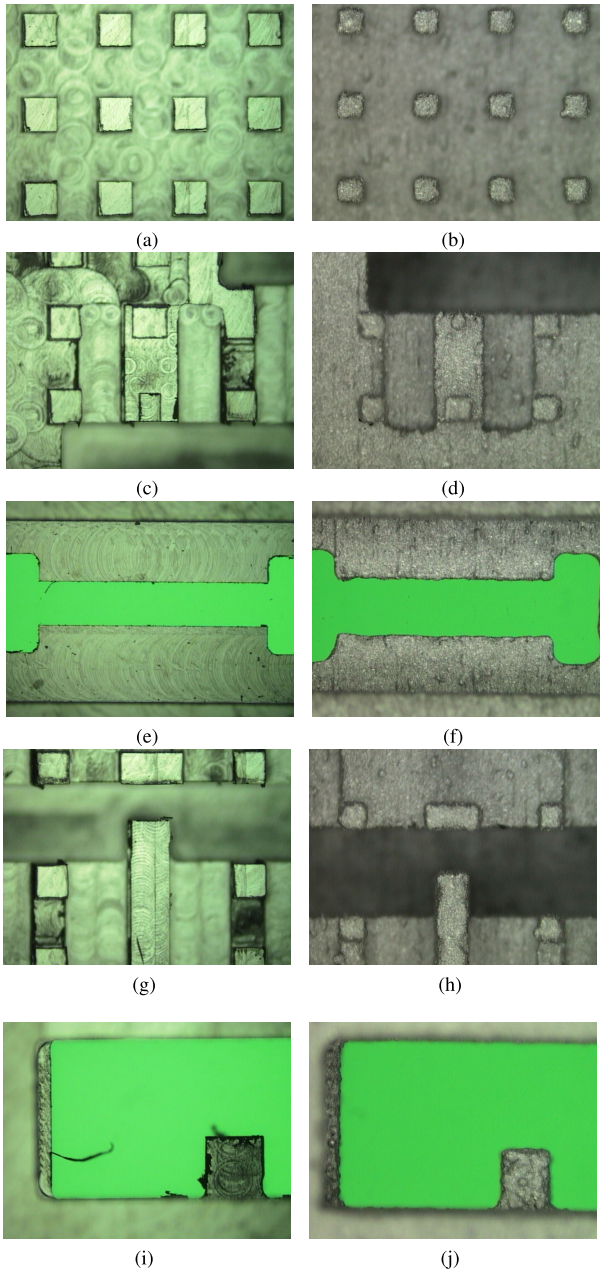

FIGURE 3. Figures in the left column: (a), (c), (e), (g) and (i) correspond to zoomed photographs of the CNC antenna using microscopy. Figures in the right column: (b), (d), (f), (h) and (j) correspond to SLS antenna captures.

FIGURE 4. Schematic of antenna parts where the relevant dimensions are indicated.

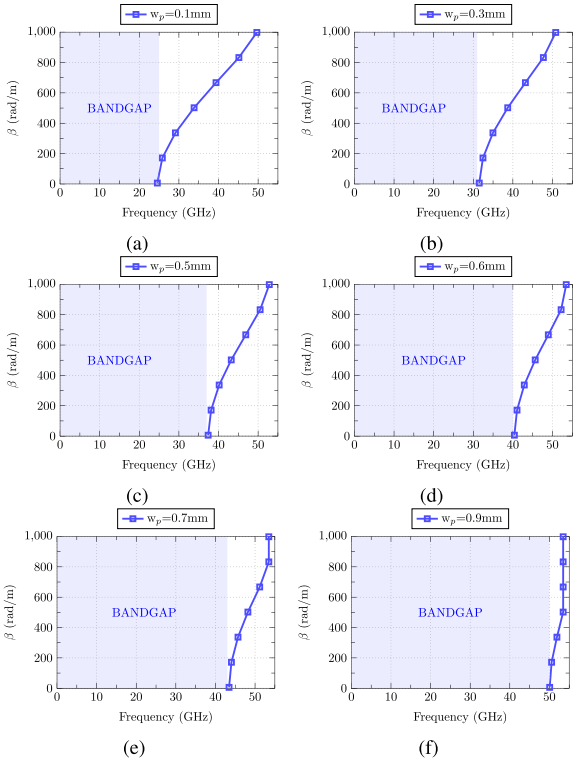

FIGURE 5. Bandgap created for different nail widths.

undesirable, is at least not dramatic since it does not spoil the performance of the gap waveguide antenna. In GW technology the nails' dimension and their periodicity create a bandgap in a certain frequency range [18], thus preventing field leakage in the operating band. Fig. 5 shows that, despite having thinner nails, the first mode appears from 37.5 GHz for a nail width of 0.5 mm. Here, with an average nail width of 0.65 mm, the stop band created by the surrounding nails ranges from 0 GHz to 40 GHz, leaving the working range from 20 GHz to 30 GHz not affected by undesired modes.

It was also studied to what extent the manufacturing deviations could have affected the general performance of the structure with respect to its ideal response. For this reason, a piece of GGW of length 3 cm (Fig. 6), with the exact dimensions of the one used in the antenna, was analyzed. Fig. 7a shows the propagation constant in the waveguide for different nail widths. It can be seen that the β-parameter is apparently similar over the frequency range. An enlarged view, though, shows a different behavior in each band (Figs. 7b and 7c).

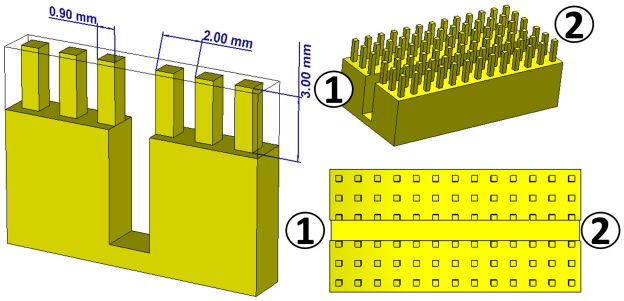

FIGURE 6. Waveguide section with the same dimensions as the GGW used in the antenna under study.

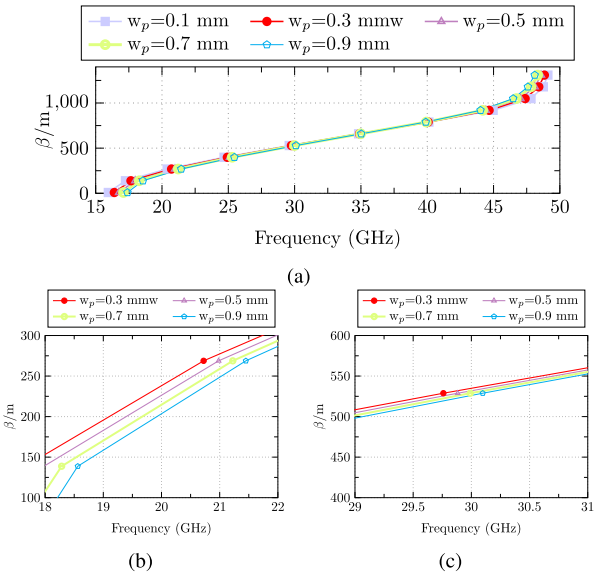

FIGURE 7. (a) Dispersion diagram in the Groove Gap Waveguide for different nail widths, (b) zoomed view centered on the low band and (c) zoomed view on the high band.

While in the high band the curves are very close for different nail widths, a larger discrepancy is observed in the low band due to its proximity to the mode cutoff frequency. This will lead to a slight shift in the reflection coefficient of the antenna in K-band, as it will be demonstrated next.

Furthermore, a roughness study is carried out to analyze its impact on the antenna efficiency. Fig. 8a indicates by means of the variable r (root-mean-square deviation roughness), how, expectedly, the higher the surface roughness the more losses appear. In fact, a transmission coefficient close to 100% is obtained on perfectly smooth surfaces and decreases to below 70% with a roughness of 50 μm. It should be noted

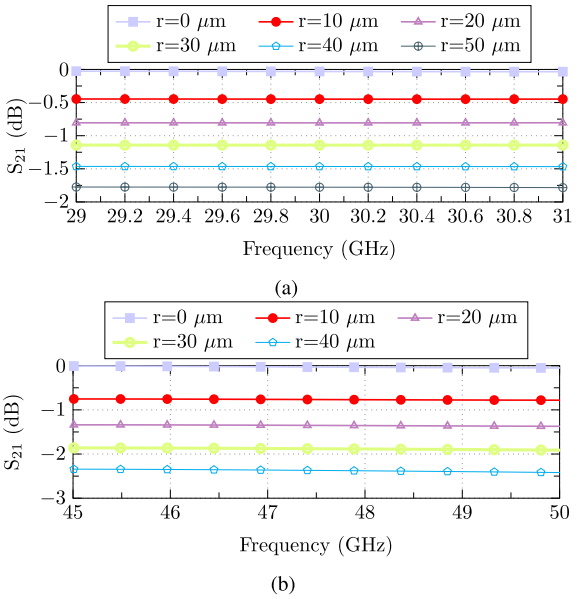

FIGURE 8. Variation of the transmission coefficient in the groove gap waveguide assuming different surface roughness (r) for: (a) Ka-band and (b) Q-band.

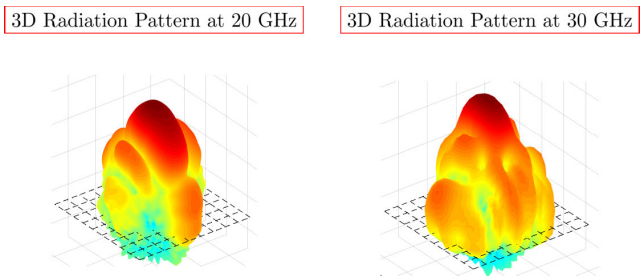

FIGURE 9. Measured 3D radiation patterns for the SLS antenna in each working band.

that such roughness may have a greater impact on insertion loss as the frequency increases. To check this, at least from a theoretical point of view, Fig. 6 has been scaled up by a factor 0.5 and simulated its response at higher frequencies. It is easily verified, as expected, that the same absolute values of roughness in a smaller piece drastically affect the wave propagation, increasing its losses (Fig. 8b).

V. EXPERIMENTAL RESULTS

The study presented here assesses the viability of SLS manufacturing by comparing the electrical performance of two identical antennas constructed with different techniques. Both antennas are shown in Fig. 1a without the lid. One prototype has been manufactured using SLS and the other one has been fully built in-house by CNC milling technique. Both antennas have been measured in the same environment and during the same period of time. As mentioned above, a mechanized and already validated prototype will be used as a reference framework to analyze the capabilities and limitations of SLS manufacture.

The novel feature of this antenna is its ability to operate in two non-adjacent bands, as 3D-measured patterns in Fig. 9

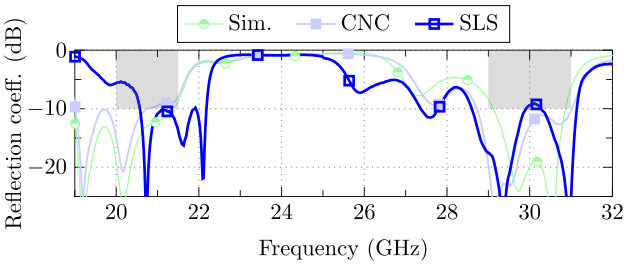

FIGURE 10. Experimental measurement of the reflection coefficient of each antenna and simulation.

demonstrates. Due to its nature, potential deviations in manufacturing can be very critical and affect its overall performance. This aspect is clearly identified in Fig. 10 where the reflection coefficient of the SLS prototype is highlighted in dark blue. With a softer color curve, the reflection coefficient of the CNC antenna is also shown for comparison purposes. Clearly, there is a deviation of the response towards higher frequencies in the low band (K-band), and the high band (Ka-band) has been more robust against manufacturing deviations. The dual-band capability remains intact, however, and two operating bands with a bandwidth greater than 1 GHz are measured in each case. Consistent with these results, the radiation patterns shown below are those corresponding to those frequency ranges where the antenna is well matched.

First, the radiation patterns measured for the SLS antenna in the K-band are shown in Fig. 11. There, the average measured directivity is 16 dBi and the antenna efficiency is close to 70%. Also, the radiation patterns measured in the Ka-band are shown in Fig. 12. Again, good frequency-stable patterns, consistent with uniform antenna illumination, are presented. Similarly, the measured antenna efficiency is antenna efficiency is close to 70% as in the low-band. However, being an all-metal antenna, high radiation efficiency is yet obtained. Finally, the radiation patterns measured for both prototypes in the two main cuts and in center frequencies of both operating bands are superimposed in Fig. 13. It is verified that, with slight deviations, the patterns show a good agreement.

Besides, Table 2 reviews some relevant papers published in recent years. All these contributions work in K or Ka band and respond to different antennas types (horns, lenses, slotted waveguides) manufactured using 3D printing techniques. Note that, beyond their physical dimensions or the particularities of each design, it can be observed that efficiencies below 60% are reported. These publications generally point to surface roughness as a key factor, among others, for their low efficiency. Specifically, the work presented in [23], which deals with a fabricated SLM horn antenna, was able to experimentally quantify the actual roughness by using a profilometer, previously used in other works by the same authors [27].

For further clarity, the most relevant results of the SLS antenna performance are compared in a table with those obtained by the same array in CNC (Table 3). It can be seen that the directivity values in both cases are similar.

TABLE 2. Comparison of the proposed SLS dual-band antenna array with recently published works in 3-D printed technology.

Previous works	Aperture (λ^2)	Working-Band(s)	3D-technique	Peak Gain	Rad. Efficiency
[19]	17 × 17	K & Ka	Selective Laser Meltering (SLM)	30.7 dBi	≈ 38%
[20]	n/a	Ku	Direct Metal Laser Sintering (DMLS)	15 dBi	n/a
[21]	1 x 1	Ku & V	SLM	12 dBi and 25 dBi	n/a
[22]	2 × 2	K	SLM	13.23 dBi	n/a
[23]	6.7 x 6.7	K	SLA & SLM	23 dBi	≈ 57.7%
[24]	1 x 1	Ka	DMLS	13.5 dBi	n/a
[25]	3 x 3	K	Polymer Jetting (Polyjet)	24.5 dBi	n/a
[26]	2.6 x 2.6	Ka	Polyjet	21.1 dBi	≈ 49%
This work	5×5	K & Ka	SLS	15 dBi and 17.8 dBi	≈ 69%

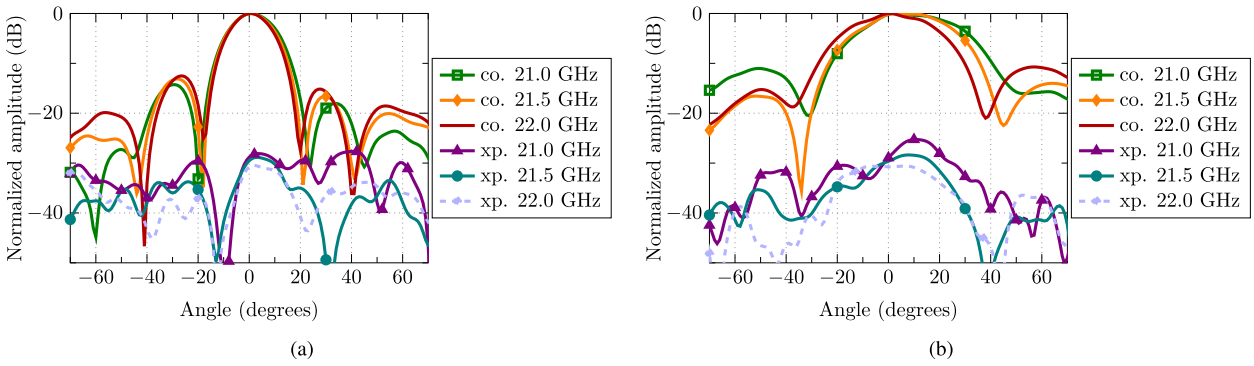

FIGURE 11. Measured radiation patterns of the SLS antenna for several frequencies in the K-band: (a) XZ-plane and (b) YZ-plane.

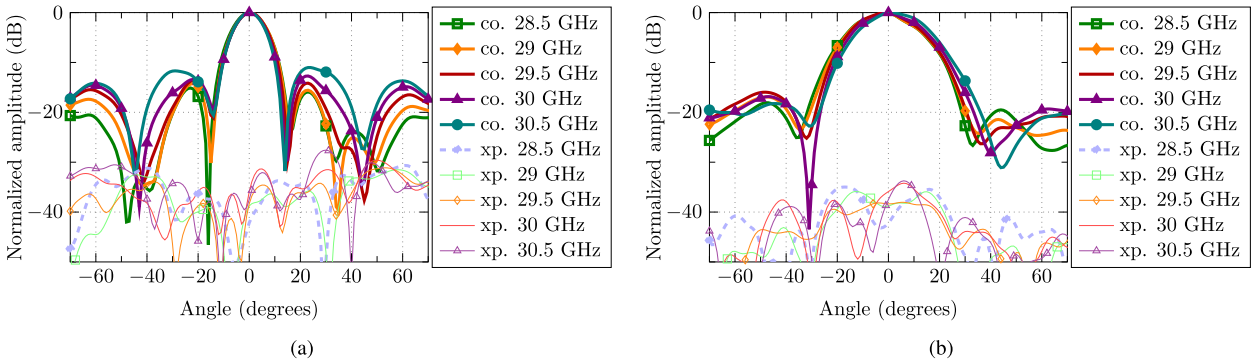

FIGURE 12. Measured radiation patterns of the SLS antenna for several frequencies in the Ka-band: (a) XZ-plane and (b) YZ-plane.

In addition, although the maximum antenna efficiency has decreased by 15% compared to the mechanized prototype, this should not be surprising due to the roughness, imperfections and manufacturing deviations already discussed in Section III. These are acceptable efficiency values considering the cost and weight savings of the SLS antenna, and remain still above those achieved by non-fully metallic antenna solutions. Finally, Fig. 14, shows for different frequencies, within both operating bands, the measured directivities, gains and radiation efficiencies.

VI. DISCUSSION

A critic comparison of the measurements and their connection to fabrication techniques are discussed below.

First of all, it must be said that the results are satisfactory because of several reasons: the cost of the piece is actually much lower in the additive technique with respect to the machined piece. In this specific case the total cost of the piece with additive technology was 430 €, being the cost of the machined piece four times higher. Obviously the costs of a piece with additive manufacturing can be higher depending on the tolerances required, but in any case the costs of the AM with respect to the subtractive manufacturing (SM) are very competitive. In addition, manufacturing times are also lower, as the piece was manufactured in less than 24 hours in AM.

In contrast, the experimental results also shed some light on this comparison. It is demonstrated that the CNC prototype works objectively better than the SLS. Although the impedance bandwidth is similar, there has been a low band shift as shown in Fig. 10. In addition to this, the most important factor to consider is that the roughness, visible in the SLS prototype in Fig. 3, makes the antenna efficiency lower.

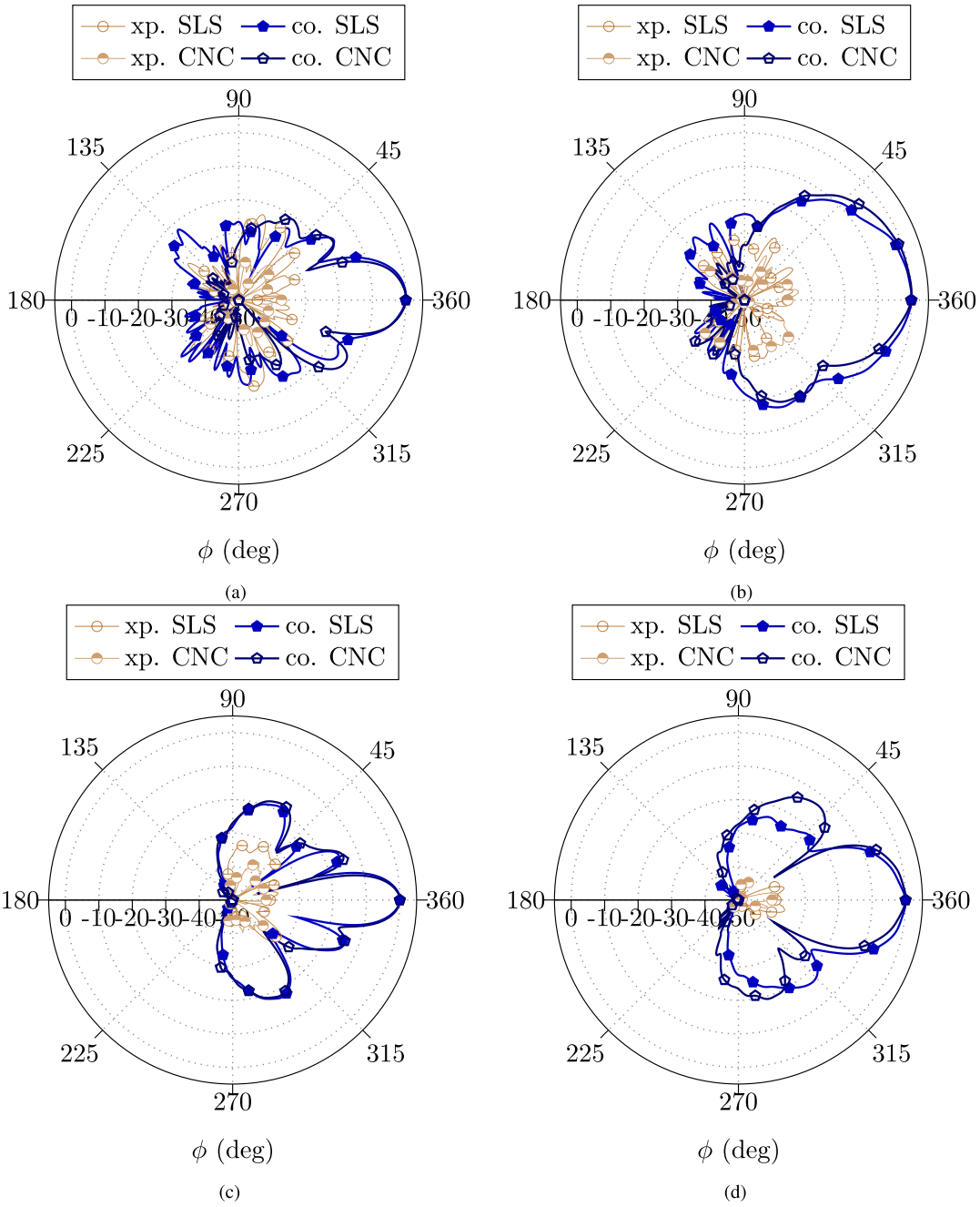

FIGURE 13. Comparison of measured radiation copolar (co.) and crosspolar (xp.) patterns on both prototypes in both working bands: (a) XZ-plane at K band, (b) YZ-plane at K band, (c) XZ-plane at Ka-band, and (d) YZ-plane at Ka-band.

Antenna efficiency goes from above 80% in the CNC to close to 70% in the SLS. While these are still good values and certainly above of those reachable by non-fully metallic antenna, it is an aspect to be considered in the design. For example, electromagnetic simulators such as CST, allow to simulate the structures with a certain surface roughness, which would be useful to make calculations for future pieces.

The metrology table also reveals that the tolerance of the heights (i.e. in Z-axis) is very similar in CNC and SLS with deviations below 0.1 mm. It is along the X-Y axes where the CNC is more precise than the SLS technique, especially for small objects.

Finally, the main conclusion that can be drawn from this research is that antennas manufactured with SLS technology are technically feasible, being their greatest strengths their low cost, low manufacturing time and low weight compared with SM technique. Besides, the experimental performance shows a good agreement with simulations, though inferior to that obtained with the prototype in CNC. Also, it must be emphasized that the use of additive technology allows the design of complicated bends that with SM will be difficult

TABLE 3. Antenna comparison performance.

	SLS Antenna		CNC Antenna	
	K-band	Ka-band	K-band	Ka-band
Total Eff. (max)	71%	73%	85%	88%
Total Eff. (mean)	>69%	>68%	>80%	>81%
Directivity (mean)	16 dBi	19 dBi	17 dBi	19 dBi
Gain (mean)	14.6 dBi	17.4 dBi	16.1 dBi	18.2 dBi

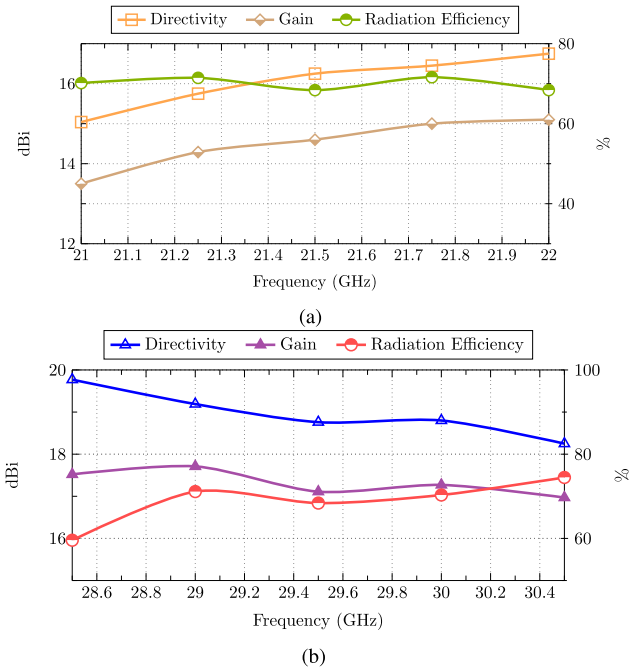

FIGURE 14. Measured directivity and gain in the SLS antenna for both bands.

or impossible to fabricate. Presumably, the growing demand and the continuous development of SLS technique will most likely improve the weak points found in this work, to become an even stronger alternative to SM in the near future.

VII. CONCLUSION

This work assesses the performance of a dual-band antenna operating in K and Ka bands, manufactured with the novel SLS technique and benchmarked with a mechanized antenna. It has been demonstrated by means of a metrological study that the manufacturing tolerances coincide with those provided by the manufacturer. In addition, the SLS technique offers more versatility for intricate designs that are difficult to fabricate with CNC. While SLS still has challenges to overcome, such as avoiding excessively rough surfaces or achieving the manufacturing tolerances offered by traditional techniques to date, it is a technique to be considered in the near future as a truly competitive alternative for fast manufacturing and low-cost flat panel antennas.

REFERENCES

[1] K. Lomakin, T. Pavlenko, M. Sippel, G. Gold, K. Helmreich, M. Ankenbrand, N. Urban, and J. Franke, "Impact of surface roughness on 3D printed SLS horn antennas," in *Proc. 12th Eur. Conf. Antennas Propag. (EuCAP)*, 2018, pp. 1–4, doi: 10.1049/cp.2018.1235.

[2] H. Yao, S. Sharma, R. Henderson, S. Ashrafi, and D. MacFarlane, "Ka band 3D printed horn antennas," in *Proc. Texas Symp. Wireless Microw. Circuits Syst. (WMCS)*, Mar. 2017, pp. 1–4.

[3] Y. Li, L. Ge, J. Wang, S. Da, D. Cao, J. Wang, and Y. Liu, "3-D printed high-gain wideband waveguide fed horn antenna arrays for millimeter-wave applications," *IEEE Trans. Antennas Propag.*, vol. 67, no. 5, pp. 2868–2877, May 2019.

[4] G. P. Le Sage, "3D printed waveguide slot array antennas," *IEEE Access*, vol. 4, pp. 1258–1265, 2016.

[5] J. Tak, A. Kantemur, Y. Sharma, and H. Xin, "A 3-D-printed W-band slotted waveguide array antenna optimized using machine learning," *IEEE Antennas Wireless Propag. Lett.*, vol. 17, no. 11, pp. 2008–2012, Nov. 2018.

[6] S.-G. Zhou, G.-L. Huang, and T.-H. Chio, "A lightweight, wideband, dual-circular-polarized waveguide cavity array designed with direct metal laser sintering considerations," *IEEE Trans. Antennas Propag.*, vol. 66, no. 2, pp. 675–682, Feb. 2018.

[7] G.-L. Huang, S.-G. Zhou, T.-H. Chio, and T.-S. Yeo, "Fabrication of a high-efficiency waveguide antenna array via direct metal laser sintering," *IEEE Antennas Wireless Propag. Lett.*, vol. 15, pp. 622–625, 2016.

[8] M. Ferrando-Rocher, J. I. Herranz-Herruzo, A. Valero-Nogueira, and B. Bernardo-Clemente, "Performance assessment of gap-waveguide array antennas: CNC milling versus three-dimensional printing," *IEEE Antennas Wireless Propag. Lett.*, vol. 17, no. 11, pp. 2056–2060, Nov. 2018.

[9] D. Helena, A. Ramos, T. Varum, and J. N. Matos, "Antenna design using modern additive manufacturing technology: A review," *IEEE Access*, vol. 8, pp. 177064–177083, 2020.

[10] M. Ferrando-Rocher, J. I. Herranz-Herruzo, A. Valero-Nogueira, and M. Baquero-Escudero, "Dual-band single-layer slot array antenna fed by K/Ka-band dual-mode resonators in gap waveguide technology," *IEEE Antennas Wireless Propag. Lett.*, vol. 20, no. 3, pp. 416–420, Mar. 2021.

[11] P.-S. Kildal, E. Alfonso, A. Valero-Nogueira, and E. Rajo-Iglesias, "Local metamaterial-based waveguides in gaps between parallel metal plates," *IEEE Antennas Wireless Propag. Lett.*, vol. 8, pp. 84–87, 2009.

[12] E. Rajo-Iglesias and P.-S. Kildal, "Groove gap waveguide: A rectangular waveguide between contactless metal plates enabled by parallel-plate cut-off," in *Proc. 4th Eur. Conf. Antennas Propag.*, Apr. 2010, pp. 1–4.

[13] A. J. Sáez, A. Valero-Nogueira, J. I. Herranz, and B. Bernardo, "Single-layer cavity-backed slot array fed by groove gap waveguide," *IEEE Antennas Wireless Propag. Lett.*, vol. 15, pp. 1402–1405, 2016.

[14] M. Ferrando-Rocher, A. Valero-Nogueira, J. I. Herranz-Herruzo, and J. Teniente, "60 GHz single-layer slot-array antenna fed by groove gap waveguide," *IEEE Antennas Wireless Propag. Lett.*, vol. 18, no. 5, pp. 846–850, May 2019.

[15] M. Baquero-Escudero, A. Valero-Nogueira, M. Ferrando-Rocher, B. Bernardo-Clemente, and V. E. Boria-Esbert, "Compact combline filter embedded in a bed of nails," *IEEE Trans. Microw. Theory Techn.*, vol. 67, no. 4, pp. 1461–1471, Apr. 2019.

[16] M. Ferrando-Rocher, A. Valero-Nogueira, and J. I. Herranz-Herruzo, "New feeding network topologies for high-gain single-layer slot array antennas using gap waveguide concept," in *Proc. 11th Eur. Conf. Antennas Propag. (EUCAP)*, Mar. 2017, pp. 1654–1657.

[17] M. Ferrando-Rocher, A. Valero-Nogueira, J. I. Herranz-Herruzo, A. Berenguer, and B. Bernardo-Clemente, "Groove gap waveguides: A contactless solution for multilayer slotted-waveguide array antenna assembly," in *Proc. 10th Eur. Conf. Antennas Propag. (EuCAP)*, Apr. 2016, pp. 1–4.

[18] M. Ferrando-Rocher, "Gap waveguide array antennas and corporate-feed networks for mm-wave band applications," Ph.D. dissertation, Dept. Commun., Universitat Politècnica de València, Valencia, Spain, 2018.

[19] X. Zhu, B. Zhang, and K. Huang, "A *K*/*Ka*-band dielectric and metallic 3D printed aperture shared multibeam parabolic reflector antenna for satellite communication," *Int. J. RF and Microw. Comput.-Aided Eng.*, vol. 30, no. 7, Jul. 2020, Art. no. e22216.

[20] A. Guennou-Martin, Y. Quéré, E. Rius, L. Fourtinon, C. Person, G. Lesueur, and T. Merlet, "Design and manufacturing of a 3-D conformal slotted waveguide antenna array in Ku-band based on direct metal laser sintering," in *Proc. IEEE Conf. Antenna Meas. Appl. (CAMA)*, Oct. 2016, pp. 1–4.

[21] G. Addamo, O. A. Peverini, F. Calignano, D. Manfredi, F. Paonessa, G. Virone, and G. Dassano, "3-D printing of high-performance feed horns from Ku-to V-bands," *IEEE Antennas Wireless Propag. Lett.*, vol. 17, no. 11, pp. 2036–2040, Nov. 2018.

[22] B. Zhang, Y.-X. Guo, H. Sun, and Y. Wu, "Metallic, 3D-printed, K-band-stepped, double-ridged square horn antennas," *Appl. Sci.*, vol. 8, no. 1, p. 33, Dec. 2017.
[23] B. Zhang, L. Wu, Y. Zhou, Y. Yang, H. Zhu, F. Cheng, Q. Chen, and K. Huang, "A K-band 3-D printed focal-shifted two-dimensional beam-scanning lens antenna with nonuniform feed," *IEEE Antennas Wireless Propag. Lett.*, vol. 18, no. 12, pp. 2721–2725, Dec. 2019.
[24] I. Agnihotri and S. K. Sharma, "Design of a 3D metal printed axial corrugated horn antenna covering full Ka-band," *IEEE Antennas Wireless Propag. Lett.*, vol. 19, no. 4, pp. 522–526, Apr. 2020.
[25] H. Xin and M. Liang, "3-D-printed microwave and THz devices using polymer jetting techniques," *Proc. IEEE*, vol. 105, no. 4, pp. 737–755, Apr. 2017.
[26] Y. Li, L. Ge, M. Chen, Z. Zhang, Z. Li, and J. Wang, "Multibeam 3-D-printed Luneburg lens fed by magnetoelectric dipole antennas for millimeter-wave MIMO applications," *IEEE Trans. Antennas Propag.*, vol. 67, no. 5, pp. 2923–2933, May 2019.
[27] B. Zhang, Z. Zhan, Y. Cao, H. Gulan, P. Linnér, J. Sun, T. Zwick, and H. Zirath, "Metallic 3-D printed antennas for millimeter- and submillimeter wave applications," *IEEE Trans. THz Sci. Technol.*, vol. 6, no. 4, pp. 592–600, Jul. 2016.

MIGUEL FERRANDO-ROCHER (Member, IEEE) was born in Alcoy, Spain. He received the M.Sc. and Ph.D. degrees in telecommunication engineering from the Universitat Politècnica de València (UPV), Valencia, Spain, in 2012 and 2018, respectively. In 2012, he joined the Complex Radiation Systems Team, Institute of Electronics and Telecommunications Rennes, France, as a Researcher, where he was involved in reflectarray antennas for satellite applications in collaboration with Thales Alenia Space, Paris, France. Since 2013, he has been with the Antennas and Propagation Laboratory, Institute of Telecommunications and Multimedia Applications, UPV. In 2016, he joined the Chalmers University of Technology, Gothenburg, Sweden, as a Guest Researcher. Since September 2019, he is an Assistant Professor with the Department of Physics, Systems Engineering and Signal Theory, University of Alicante. His research activity is also developed with the Microwave and Applied Computational Electromagnetics Group (GMECA). His current research interests include satellite communication (SATCOM) on-the-move, high-gain antennas and arrays, gap waveguide (GW) technology, and millimeter-wave components. He was a recipient of the Extraordinary Prize for Doctoral Theses from the Polytechnic University of Valencia, in 2020, the AIRBUS Defence and Space Award, in 2019, and the URSI Conference Best Student Paper Award, in 2017. He received the Erasmus Grant to study with Ghent University, Ghent, Belgium, in 2010.

JOSE IGNACIO HERRANZ-HERRUZO (Member, IEEE) was born in Valencia, Spain, in 1978. He received the M.S. and Ph.D. degrees in telecommunication engineering from the Universitat Politècnica de València (UPV), Valencia, in 2002 and 2015, respectively. In 2002, he joined the Antennas and Propagation Laboratory, Institute of Telecommunications and Multimedia Applications (UPV). In 2005, he became an Assistant Professor with the Communications Department (UPV), where he has been an Associate Professor, since 2019. His current research interests include the numerical modelling and design of waveguide slot arrays, and the application of gap waveguide technology to the design of microwave and millimeter-wave antennas and components.

ALEJANDRO VALERO-NOGUEIRA (Senior Member, IEEE) was born in Madrid, Spain, in 1965. He received the degree in telecommunication engineering from the Universidad Politécnica de Madrid, Madrid, in 1991, and the Ph.D. degree in telecommunication from the Universitat Politècnica de València, Valencia, Spain, in 1997. In 1992, he joined the Departamento de Comunicaciones, Universitat Politècnica de València, where he is currently a Full Professor. In 1999, he was on leave from the ElectroScience Laboratory, The Ohio State University, Columbus, OH, USA, where he was involved in fast solution methods in electromagnetics (EMs) and conformal antenna arrays. His current research interests include computational EMs, waveguide slot arrays, gap waveguides (GW), theory of characteristic modes, and automated antenna design procedures.

BERNARDO BERNARDO-CLEMENTE was born in Valencia, Spain, in 1972. He received the degree in telecommunication engineering from the Universitat Politècnica de València, Valencia, Spain, in 2003, where he is currently pursuing the Ph.D. degree in telecommunication. Since 2005, he has been with the Instituto de Telecomunicaciones y Aplicaciones Multimedia (ITEAM), Universitat Politècnica de València. His current research interests include antenna measurement, antenna fabrication, and near to far-field transformation.